

Neutron Multigroup Constant Sets of Moderator Materials for Design of Low-Energy Neutron Sources

Yutaka Abe and Nobuhiro Morishima

Department of Nuclear Engineering, Kyoto University
Yoshida, Sakyo-ku, Kyoto 606-8501, Japan
e-mail: yutaka_abe@nucleng.kyoto-u.ac.jp (Yutaka Abe)

For design assessment of low-energy neutron sources, neutron multigroup constant sets (energy-averaged cross sections) are developed, which consist of 36 sets of multigroup constants for liquid ^4He , H_2 , D_2 , CH_4 , H_2O and D_2O and solid CH_4 at many different temperatures. The neutron energy range between $0.1 \mu\text{eV}$ and 10 MeV are divided into 140 energy groups at equal logarithmic intervals. The angular distribution of scattered neutrons is represented by the expansion in Legendre polynomials up to order 3. The multigroup constants at energies below 10 eV are generated using physical models of a double-differential scattering cross section for the moderator materials, which are newly developed for describing low-energy neutron scattering in terms of the general considerations of molecular dynamics and structures inherent in liquid and solid phases.

Most of the calculated cross-section results are compared with many experimental measurements, both double-differential and total, at various material temperatures and neutron energies. Availability of the constant sets are demonstrated by the multigroup neutron transport analyses for production of ultra-cold ($\sim 0.3 \mu\text{eV}$), cold ($\sim 2 \text{ meV}$) and thermal ($\sim 25 \text{ meV}$) neutrons. Features of the multigroup constant sets for each moderator material and typical results of low-energy neutron production are reported in the present study.

1 Introduction

Although a variety of moderators have been actually used for low-energy neutron sources, most of them are hydrogenous liquids because of the following advantages: large scattering cross section leading to rapid moderation and small source volume; good removal of neutron kinetic energy by excitation of molecular motions; favorable refrigeration requirements due, in some liquids, to low melting and boiling points; and much less technical problems as compared with solid moderators at the time of heat dissipation and radiation damage. Hence, moderator materials to be taken up below are liquid H_2 , D_2 , CH_4 , H_2O and D_2O , together with solid CH_4 and liquid ^4He . The last two materials are selected from the viewpoints of an efficient solid moderator for production of an intense cold neutron beam and a specific liquid moderator for an ultracold neutron source.

At present, available experimental data for the moderator materials are very limited in comprehensive tabulations and interpolations. Consequently, scattering cross section models are newly developed to describe major features of neutron scattering in the liquid and solid moderators for neutron energies E between $0.1 \mu\text{eV}$ and 10 eV [1, 2]. This aims at generating a cross section library available for research and development of advanced neutron sources to produce ultracold ($\sim 0.3 \mu\text{eV}$), very cold ($\sim 10 \mu\text{eV}$) and cold ($\sim 2 \text{ meV}$) neutrons. By use of the cross section models, together with an evaluated nuclear data file for $E \geq 10 \text{ eV}$, a total of 36 sets of 140-group constants (averaged cross sections over the energies of each group) are systematically generated in the energy range between $0.1 \mu\text{eV}$ and 10 MeV . Accordingly, it becomes possible to evaluate slowing-down of fission/spallation neutrons and thermalization to thermal and cold neutrons, including the production and storage of ultracold neutrons.

Table 1. Group constant sets for moderator materials at temperatures.

Material	N_s	T	N_m in order of T	$\sigma_{a,th}$	σ_{fr}
Liquid ^4He	11	0.1,0.3,0.5,0.6	2.189 in common	2.34×10^{-7}	0.760
		0.7,0.8,0.9,1.0	2.189 in common		
		1.5,2.0,2.5	2.190,2.197,2.180		
Liquid para- H_2	2	14.0,20.4	2.30,2.11	0.665	41.0
Liquid ortho- H_2	2	14.0,20.4	2.31,2.12	0.665	41.0
Liquid normal- H_2	2	14.0,20.4	2.31,2.12	0.665	41.0
Liquid para- D_2	2	18.7,23.6	2.61,2.45	1.04×10^{-3}	6.80
Liquid ortho- D_2	2	18.7,23.6	2.61,2.45	1.04×10^{-3}	6.80
Liquid normal- D_2	2	18.7,23.6	2.61,2.45	1.04×10^{-3}	6.80
Solid CH_4	3	20.4,50.0,90.7	1.99,1.92,1.83	1.33	86.8
Liquid CH_4	2	90.7,111.7	1.70,1.59	1.33	86.8
Liquid H_2O	4	278,300,325,350	3.35,3.33,3.30,3.26	0.665	44.8
Liquid D_2O	4	278,300,325,350	3.35,3.33,3.30,3.26	1.04×10^{-3}	10.6

where N_s (number of sets), T (K), N_m ($\times 10^{22}$ molecules cm^{-3}), $\sigma_{a,th}$ (b molecule $^{-1}$) at $E_{th} = 25$ meV and σ_{fr} (b molecule $^{-1}$) at $E = 10$ eV.

2 Generation of Multigroup Constant Sets

The high-energy part for $E \geq 1$ eV (energy group $g \leq 70$) and the low-energy part for $E \leq 10$ eV ($g \geq 61$) are made up separately and then combined into one set. The overlapping energy region between 1 and 10 eV is prepared to make a gradual transition between the two parts: this is made using the expression of $W \times$ (the high-energy part) + $(1 - W) \times$ (the low-energy part) with the weight $W = (E - 1)/9$ for $E = 1 - 10$ eV. The resulting group constants are examined with total scattering cross sections, integral quantities (e.g., averaged scattering angle and averaged energy transfer) and neutron energy spectra. The high-energy part is produced using the Japanese evaluated nuclear data library JENDL-3.3[3] and the nuclear data processing program NJOY[4]. The low-energy part is created by use of double-differential scattering cross section models developed theoretically for liquid and solid moderator materials. Low-energy neutron scattering by molecular dynamics inherent in each material is generally described and the calculated cross-section results are compared with many experimental measurements, both double-differential and total, at many different temperatures and neutron energies. Slowing-down and thermalization properties are analyzed by calculating neutron energy spectra for moderator models in relatively simple geometries such as an infinite slab and a finite slab surrounded by a vacuum. All the results are reported in research papers on scientific journal: liquid ^4He [5, 6, 7, 8], liquid H_2 [9, 10, 11], liquid D_2 [12, 13, 14], solid CH_4 [15, 16, 17], liquid CH_4 [15, 16, 17], liquid H_2O [18, 19], and liquid D_2O [19, 20].

Table 1 summarizes the group constant sets generated for the seven different materials at various temperatures, mostly between melting and boiling points. For liquid H_2 and D_2 , two sorts of sets, distinguished by the spin states of para and ortho, are prepared in order to make up a mixture with an arbitrary-chosen para:ortho ratio. In Table 1, σ_{fr} is the free atom cross section (b molecule $^{-1}$) at $E = 10$ eV and $\sigma_{a,th}$ is the absorption cross section (b molecule $^{-1}$) at a thermal neutron energy $E_{th} = 25$ meV. By use of $\sigma_{a,th}$, an absorption (radiative capture) cross section $\sigma_a(E)$ as a function of E is defined by $\sigma_a(E) = \sigma_{a,th} \sqrt{E_{th}/E}$. One exception is $\sigma_a(E)$ of liquid ^4He which is given by $\sigma_a(E) = 1/(N_m \tau_\beta v)$ due to the neutron β -decay with a lifetime $\tau_\beta = 885.7$ s, together with the number density N_m of molecules (molecules cm^{-3}) and a neutron speed $v = 2.20 \times 10^5 \sqrt{E/E_{th}}$ cm s $^{-1}$. For reference, the value of N_m for each

material is also presented as an equilibrium or theoretical value at given temperature since it is required for making up macroscopic cross section tables for neutron transport analyses. The group constant sets have the following structure and property:

1. Neutron energy range between $0.1 \mu\text{eV}$ and 10 MeV ,
2. A total of 140 energy groups at equal logarithmic energy intervals(i.e. 10 groups per energy decade),
3. Expansion of the angular distribution of scattered neutrons in Legendre polynomials up to order 3,
4. Weighting energy spectrum of a neutron flux by a combination of Maxwellian, $1/E$ and fission spectra as a function of E ,
5. Microscopic cross sections(b molecule⁻¹) in ANISN-type cross section tables (text form, length IHM=282, position IHT=3, groups IGM=140) though not multiplied by the Legendre factor $(2l + 1)$.

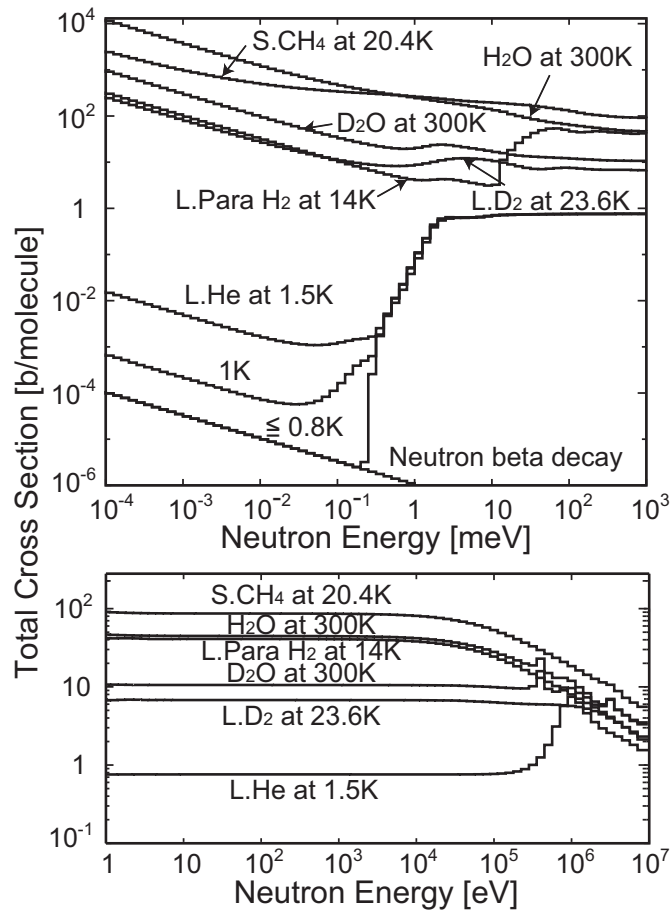


Figure 1: Total cross sections of various moderator materials at temperatures shown, together with an effective absorption cross section due to the neutron β -decay.

In addition, it is worth noting the definition of the group constants, i.e. energy-averaged scattering cross sections associated with the change of neutron energies from group g to g' ,

$$\sigma_s^l(g \rightarrow g') = 2\pi \int_{-1}^1 d \cos \theta \int_{E_g}^{E_{g-1}} dE \int_{E_{g'}}^{E_{g'-1}} dE' w_g(E) \sigma_s(E \rightarrow E', \theta) P_l(\cos \theta) \quad (l = 0, 1, \dots, L; g \text{ and } g' = 1, 2, \dots, G) \quad (1)$$

where $\sigma_s(E \rightarrow E', \theta)$ is the double-differential scattering cross section for initial and final energies, E and E' respectively, at scattering angle θ , $w_g(E)$ is the intergroup weighting spectrum, $P_l(\cos \theta)$ is the Legendre polynomial of order l , and E_{g-1} and E_g are, respectively, the upper and lower energy boundaries of energy group g and given by

$$E_g = E_0 \exp \left[-\frac{g}{G} \ln \frac{E_0}{E_G} \right] \quad (2)$$

with $E_0 = 10$ MeV, $E_G = 0.1$ μ eV, $L = 3$ and $G = 140$. Numerical methods for calculation of $\sigma_s(E \rightarrow E', \theta)$ and $\sigma_s^l(g \rightarrow g')$ are described in detail and illustrated with physical cross section models[1, 2]. The total cross sections of scattering and absorption in group g are defined as, respectively,

$$\sigma_{s,g} = \sum_{g'=1}^G \sigma_s^0(g \rightarrow g') \quad (3)$$

$$\sigma_{a,g} = \int_{E_g}^{E_{g-1}} w_g(E) \sigma_a(E) dE. \quad (4)$$

Then the total cross section for any type of neutron reaction is given by

$$\sigma_{t,g} = \sigma_{s,g} + \sigma_{a,g}. \quad (5)$$

Figure 1 shows $\sigma_{t,g}$ for various moderator materials at specified temperatures in the whole energy range from 0.1 μ eV (group 140) to 10 MeV (group 1), together with $\sigma_{a,g}$ of liquid ^4He due to the neutron β -decay.

3 Demonstration of Low-energy Neutron Production

3.1 Production and Storage of Ultracold Neutrons in Liquid ^4He

Multigroup constants of liquid ^4He are generated by using the cross-section model[6] developed for neutron scattering in liquid ^4He at temperatures between 0.1 and 4.2 K. The model describes some fundamental excitations in superfluid and normal ^4He in terms of phonon-roton (quasi-particle) excitation at temperatures below $T_\lambda = 2.172$ K and density mode (non-condensate component) excitation at all temperatures[21], together with an elastic scattering collision with a ^4He nucleus for incident energies above about 10 meV. The temperature dependence of these excitations is verified by comparison with the experimental results of scattering cross sections, both double-differential and total [5, 6]. Figure 2 shows the scattering cross section $\sigma_s^0(g \rightarrow g')$ of liquid ^4He at 0.1 and 1.5 K. The production of ultracold neutron (UCN) in liquid ^4He occurs by a single down-scattering event for a cold neutron with an incident energy of about 1 meV, because neutron with an energy of 1 meV transfers its almost entire energy and momentum to a phonon in liquid ^4He at the intersection of the free neutron dispersion curve with the phonon-roton one. The UCN production is found in Fig. 2 as a peak near the incident energy of 1.0 meV and final energy of 0.1 μ eV.

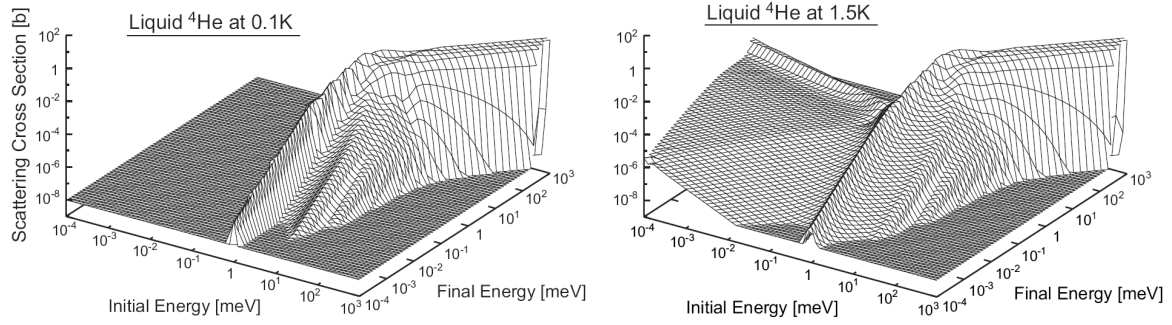


Figure 2: Scattering cross sections $\sigma_s^0(g \rightarrow g')$ of liquid ${}^4\text{He}$ at 0.1 K (left) and 1.5 K (right).

To demonstrate UCN production in liquid ${}^4\text{He}$, an UCN source is modeled as an infinite-slab geometry with a thickness of 3 m. An isotropic plane neutron source with an intensity of $2 \times 10^{10} \text{ cm}^{-2}\text{s}^{-1}$, emitting cold neutrons with a Maxwellian spectrum at 20 K, is located at left boundary of the slab, so that one half of the source neutrons enters into the slab. Boundary conditions particular to UCNs are considered, that is, there are no incoming neutrons with energies above $0.316 \mu\text{eV}$ ($1 \leq g \leq 135$) at both boundaries (i.e. vacuum boundary condition), while UCNs with energies below $0.316 \mu\text{eV}$ ($136 \leq g \leq 140$) are totally reflected at the surfaces. Neutron energy spectra calculated at an opposite side to the cold-neutron source are shown in Fig. 3, together with the Maxwellian spectrum of the cold neutron source with a neutron temperature of 20 K. Storage of UCNs is obvious especially at lower temperatures, thus yielding the UCN density of $7.7 \times 10^4 \text{ cm}^{-3}$ below 0.5 K. It is to be noted that the UCN production by down-scattering of a 1-meV neutron is almost independent of liquid temperature. On the contrary, as temperature is raised, up-scattering of an UCN becomes significant instead of disappearance by the neutron β -decay. This is due to an increase in the number of thermally-excited phonons in liquid ${}^4\text{He}$ at higher temperatures.

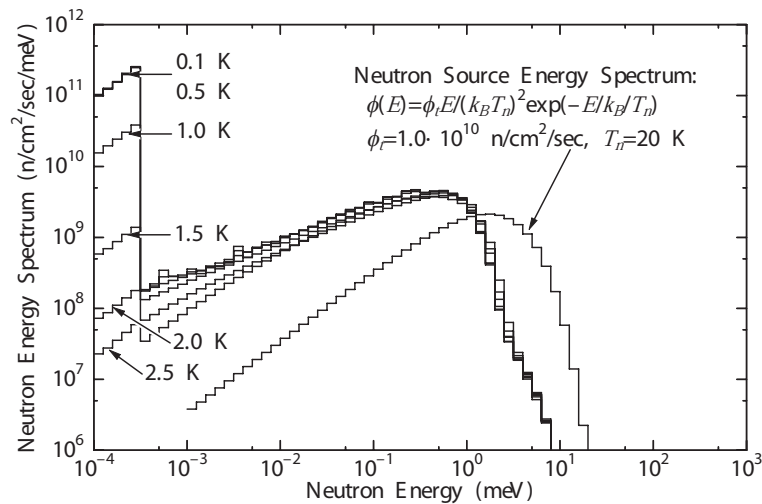


Figure 3: Neutron energy spectra for a liquid- ${}^4\text{He}$ source model at temperatures shown, together with a cold-neutron source spectrum having a Maxwellian distribution at 20 K.

3.2 Converter Characteristics of Liquid H₂ and D₂

Liquid H₂, both in the para state(anti-parallel spins of two protons) and in the ortho state(parallel spins), is efficient for producing high-density cold neutrons. This is due to the following properties: (a)a large scattering cross section, (b)a para-to-ortho(e.g. $J = 0 \rightarrow 1$) transition for free molecular rotations with energy levels $E_J = 15 \times J(J + 1)/2$ meV ($J = 0, 1, 2, \dots$) and (c)a thermal translational motion of a molecule with kinetic energies around $k_B T \sim 2$ meV where k_B is the Boltzmann constant. In order to describe low-energy neutron scattering in liquid H₂, the cross section model[9] has been developed as a generalization of the Young-Koppel model for gaseous H₂[22]. Various intermolecular motions are fully taken into account: a very short-time free-gas like translation, a short-lived vibration of about 5.3 meV due to molecular interaction, and a long-time diffusive motion with a temperature dependent diffusion coefficient. Coherent scattering in liquid para-H₂ is also included in a convolution approximation based on the experimental static structure factor. Besides, the following intramolecular motions are considered: nuclear-spin correlations, free quantized rotations of a molecule and harmonic stretching vibrations (~ 0.546 eV) of an atomic bond. A satisfactory agreement with the experimental cross section results, both double-differential and total has been found for various neutron energies and liquid temperatures [9, 11, 12]. In Fig. 4, $\sigma_s^0(g \rightarrow g')$ for liquid normal-H₂ at 14 K is shown. Since liquid normal-H₂ with a para:ortho ratio of 1:3 is mainly incoherent scatterer, it has a large scattering cross section to indicate neutron slowing down at $E >$ about 10 meV and a quasi-elastic scattering cross section at lower E , together with a up-scattering component for lower-energy neutrons to gain a kinetic energy of 15 meV by the $J = 1 \rightarrow 0$ transition. The cross-section model of liquid D₂ is also described in common with liquid H₂ except for the following points: the energy levels $E_J = 7.5 \times J(J + 1)/2$ meV from the rotation of a D₂ molecule, the vibrational energies of about 2.6 meV from an intermolecular vibration and the intramolecular vibrational energy of 386 meV, together with a very small absorption cross section for pure liquid D₂. The cross-section model of liquid D₂ is found to be in good agreement with the experimental results of cold neutron scattering cross sections, both double-differential and total [9, 12, 13, 14].

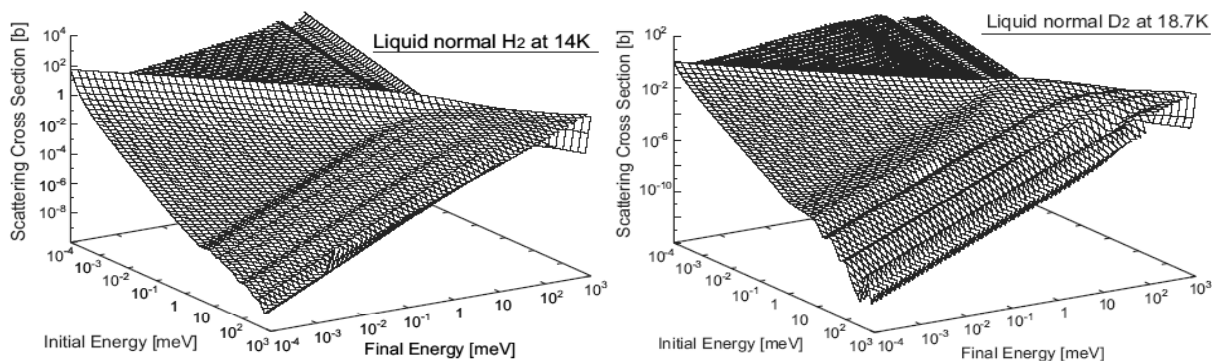


Figure 4: Scattering cross sections $\sigma_s^0(g \rightarrow g')$ of normal-H₂ at 14 K (left) and liquid normal-D₂ at 18.7 K (right).

To see converter characteristics of liquid normal-, para- and ortho-H₂ at 20.4 K, a cold-neutron source is modeled as a bare-slab geometry with a thickness a to be varied, An isotropic plane neutron source with an intensity of 2×10^{10} cm⁻²s⁻¹, emitting thermal neutrons with a Maxwellian spectrum at 300 K, is located at the left boundary. Neutron energy spectra at the right boundary are calculated by varying a so that a cold neutron flux for $E \sim 2$ meV may be maximized. The selected values of a are about 3, 2 and 2 cm for liquid para-, normal- and

ortho-H₂, respectively. The energy spectra obtained are shown in Fig. 5. A para-H₂ converter is superior in producing cold neutrons on account of the para-to-ortho transition of a H₂ molecule (i.e. an efficient down-scattering of a thermal neutron) and a small total cross section for cold neutrons below about 15 meV (i.e. a good penetrating property). It is to be noted that up-scattering of cold and lower-energy neutrons is caused by an ortho-to-para transition with an energy transfer of 15 meV and a de-excitation of intermolecular vibration with a characteristic energy of about 6 meV. This behavior may be slightly seen from Fig. 5 in terms of the shoulders of energy spectra for liquid normal- and ortho-H₂ at energies around 15 meV.

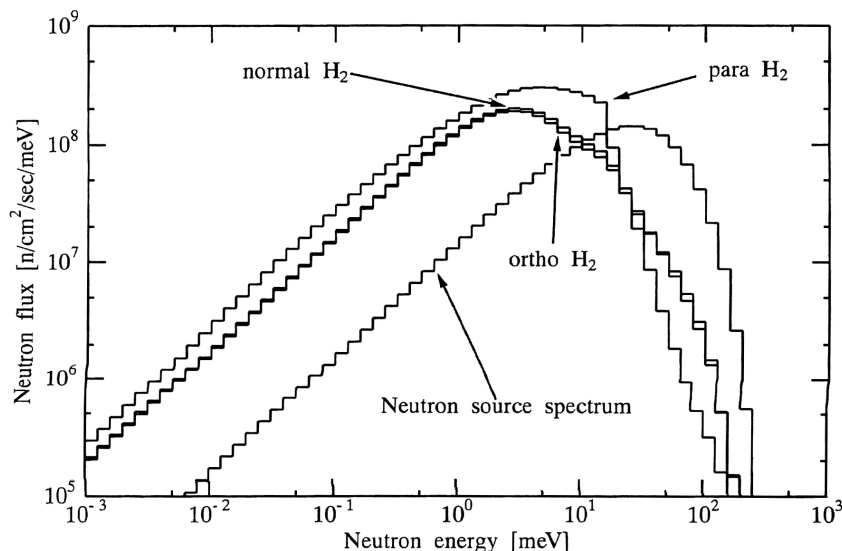


Figure 5: Neutron energy spectra for slab moderators of liquid para-, normal- and ortho-H₂ at 20.4 K, together with the Maxwellian neutron-source spectrum at 300 K.

3.3 Cold Neutron Source of Solid and Liquid CH₄ in a Thermal Neutron Field

Among various realistic hydrogenous moderators, solid CH₄ has a relatively high hydrogen-atom density that is advantageous to fast-neutron slowing-down in a narrow region with a small time spread. For thermal neutrons thus produced, there are some low-energy exchange modes, both intra- and intermolecular, for cold neutron production. A typical one is nearly free rotation of a CH₄ molecule in solid and liquid phases. By the excitation of rotational motions with energy levels $E_J = 1.3 \times J(J + 1)/2$ meV ($J = 0, 1, 2, \dots$), most of thermal neutrons are downscattered to yield cold neutrons. For intermolecular motions, low-frequency lattice vibrations in solid phase and translational vibrations in liquid phase may possibly contribute to the moderation of thermal neutrons. On the basis of these viewpoints, neutron scattering cross sections for solid CH₄ in the temperature range from 20.4 to 90.7 K and for liquid CH₄ at temperatures between 90.7 and 111.7 K are evaluated theoretically as cross-section models[15]. Major features of the cross-section models are as follows: short-time free rotation of a CH₄ molecule and long-time isotropic rotational diffusion with a temperature-dependent relaxation constant. The former is very efficient for cold neutron production by successive inelastic scatterings, while the latter gives rise to quasi-elastic scattering accompanied with very small energy transfer. The other features are the inclusion of molecular translations such as very short-time free-gas like motion, short-lived vibration of about 6.45 meV and longtime diffusion(only in the liquid phase). The intramolecular vibrations with two characteristic energies of 0.170 and 0.387 eV are also

considered. A good agreement with the experimentally-measured cross-sections, both double-differential and total, at many different temperatures is found [15]. Figure 6 shows scattering cross sections $\sigma_s^0(g \rightarrow g')$ of solid and liquid CH₄. At low temperatures quasi-elastic scattering by the molecular rotational diffusion becomes dominant while up-scattering at low energies below 1 meV is relatively suppressed. This is shown in Fig. 1 in terms of a gradual increase in $\sigma_{t,g}$ with decreasing neutron energies below 1 meV.

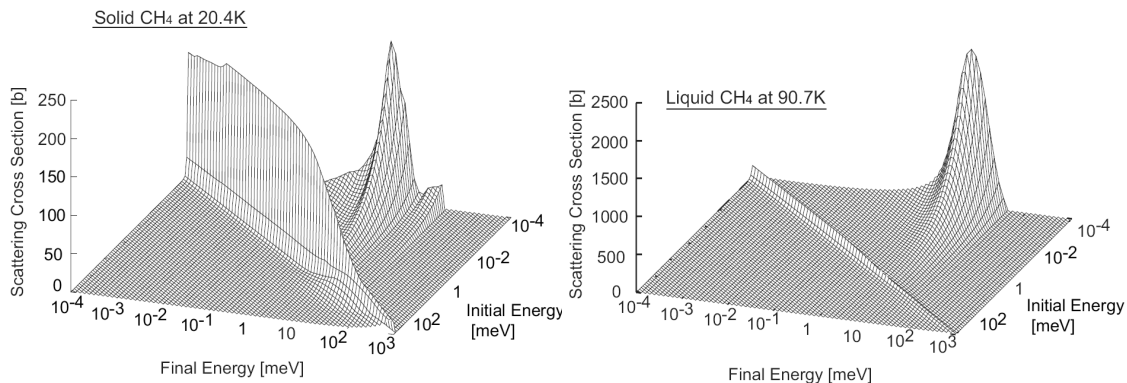


Figure 6: Scattering cross sections $\sigma_s^0(g \rightarrow g')$ of solid CH₄ at 20.4 K (left) and liquid CH₄ at 90.7 K (right).

A cold-neutron source is modeled as a slab geometry with a thickness of $D = 15$ cm. A uniformly distributed source of an intensity of $1 \text{ n cm}^{-3}\text{s}^{-1}$ is located throughout the moderator, emitting epithermal neutrons with energies of group 61 ($7.94 \text{ eV} \leq E \leq 10 \text{ eV}$). A set of neutron energy spectra at the slab center is shown in Fig. 7 in which the magnitudes are normalized in the energy region of a $1/E$ component. It is ascertained that, with increasing D more than 15 cm, there is little change of an energy spectrum in magnitude and shape. This means that almost equilibrium spectra characterizing each of the moderators are obtained for $D = 15$ cm. Since a Maxwellian plus $1/E$ spectrum is well fitted, a neutron temperature T_N and a cold-neutron gain can be determined systematically as a function of moderator temperature. Consequently, good moderating properties of solid CH₄ at 20.4 K are found especially in terms of a variation of T_N in direct proportion to moderator temperature and a good agreement of T_N with experimental results [16, 17].

3.4 Thermalization of Fission Neutrons in Liquid H₂O and D₂O

Cold and thermal neutron scattering in liquid H₂O has been described in terms of the physical cross section model[18]. The microscopic dynamics of water molecules is fully represented from very general consideration of jump diffusion, intermolecular vibration, hindered rotation and intramolecular vibration at temperatures between melting and boiling points. Furthermore, the cross-section model has been employed to treat neutron scattering by liquid D₂O[20]. Coherent neutron scattering is expressed in a convolution approximation based on the partial static structure factors for pairs of DD, DO and OO. For the double-differential and total cross sections of liquid H₂O and D₂O, satisfactory agreement with the neutron scattering experiments has been found [18, 19, 20]. It is shown that the inclusion of water molecule dynamics is essential for proper understanding and reproduction of the experimentally-observed behavior of low-energy neutron scattering. This is in marked contrast to the molecular-gas models for H₂O[23] and D₂O[24]. Figure 8 shows $\sigma_s^0(g \rightarrow g')$ for liquid H₂O and D₂O at 300 K. The following features are observed: quasi-elastic scattering components centered around initial energies below

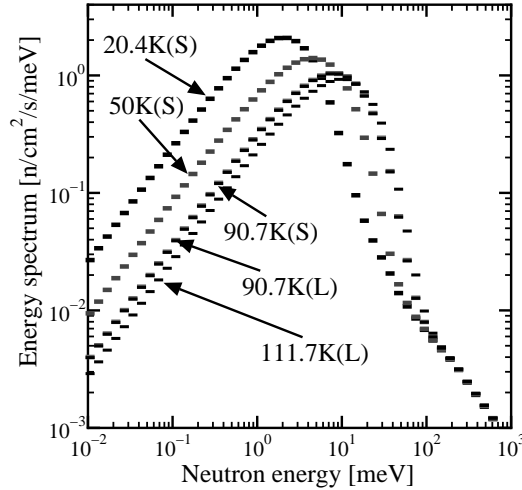


Figure 7: Neutron energy spectra for slab moderators of solid and liquid CH_4 at temperatures shown. The characters S and L, respectively, mean solid and liquid phases.

about 10 meV and up-scattering peaks for final energies $\sim 5\text{-}60$ meV by the de-excitation of intermolecular vibration and hindered rotation.

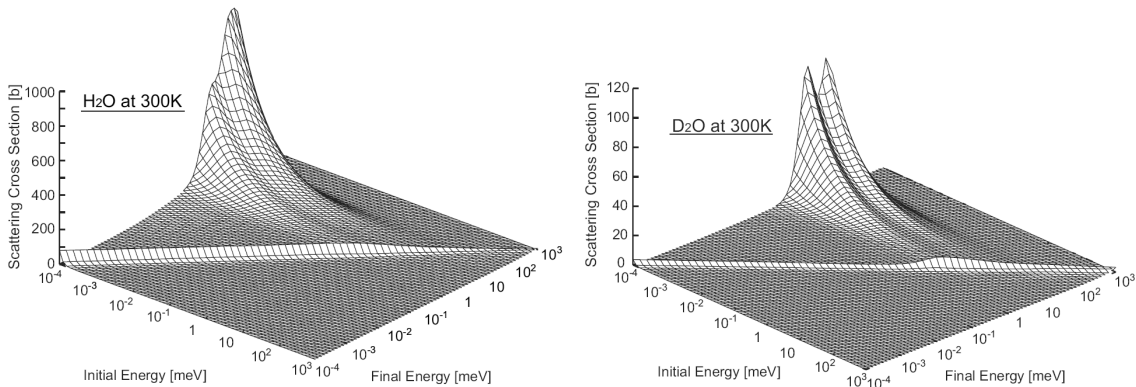


Figure 8: Scattering cross sections $\sigma_s^0(g \rightarrow g')$ of liquid H_2O at 300 K (left) and D_2O at 300 K (right).

To demonstrate thermalization of fast neutrons, infinite homogeneous mediums such as pure liquid H_2O and D_2O at 300 K, liquid D_2O containing slightly liquid H_2O (0.25, 1, 3 and 10 %), and liquid H_2O poisoned with a $1/v$ absorber (3.15 and 6.04 b H^{-1} at E_{th} , instead of 0.333 b H^{-1} for pure liquid H_2O) are prepared. Spatially-uniform neutron sources emitting fission neutrons with an average energy of 2 MeV are located in the medium. Neutron energy spectra in the whole energy range $0.1 \mu\text{eV}$ to 10 MeV are shown in Fig. 9, though normalized to the $1/E$ component around 10 eV. Moderating properties to thermal neutrons vary systematically according to the H_2O content in liquid D_2O and the poison concentration in liquid H_2O . This may also be characterized in terms of a neutron temperature and a thermal neutron gain to be estimated by a least-square fitting of a Maxwellian plus $1/E$ spectrum. A notable feature of the infinite-medium energy spectra is that there are significant non-Maxwellian deviations at varying temperatures, caused by water molecular dynamics, i.e. a jump diffusion process

with translational diffusion and intermolecular vibration, and a hindered rotation with a broad distribution of energies around 80 meV [19]. This spectral behavior is essentially in contrast to the corresponding energy spectra by molecular gas models.

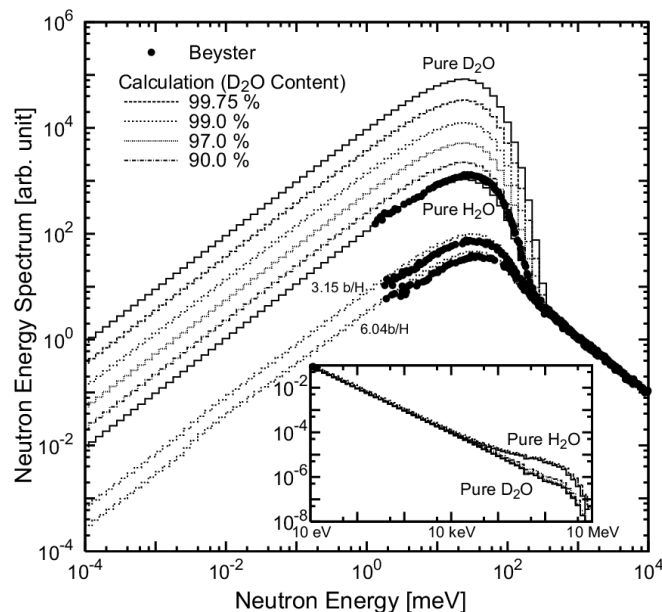


Figure 9: Infinite medium energy spectra of neutron fluxes in liquid H₂O, liquid D₂O and their mixtures at 300 K. The experimental data by Beyster [25] are shown by full circles.

4 Concluding Remarks

A total of 36 sets of multigroup constants for 6 moderator materials are developed and confirmed to be applicable in the wide range of neutron energies from 0.1 μeV (UCN) to 10 MeV (fission neutron) by the neutron multigroup transport analysis. The cross section library has been released at OECD/NEA Data Bank and RIST NUCIS [26]. The authors expect it to serve for research and development of advanced low-energy neutron sources. Optimum design of pulsed spallation neutron sources may be made in terms of low-energy neutron intensity and pulse characteristics.

Since the present multigroup library is developed as the ANISN type of 140-group constant sets, it is also necessary to generate scattering-law files for continuous energy Monte Carlo calculations. For further research, it is desirable to treat other moderating materials such as, for instance, solid CH₄ in phase II below 20.4 K, solid D₂ and solid CD₄, together with reflector and structure materials.

Acknowledgment

The authors are grateful to Mr. Y. Nagaya of JAEA for making available group-constant generation codes and Dr. Y. Edura for generating high-energy group constants.

References

- [1] N. Morishima and S. Ito: *Nucl. Instr. and Method*, **A572**, 1071 (2007).

- [2] N. Morishima: *J. Neutron Res.*, **13**, 225 (2005).
- [3] K. Shibata et al.: *J. Nucl. Sci. Technol.*, **39**, 1125 (2002).
- [4] R. E. MacFarlane and D. W. Muir: “*The NJOY Nuclear Data Processing System, Version 91*,” LA-12740-M, Los Alamos National Laboratory (1994).
- [5] N. Morishima and Y. Abe: *Nucl. Instr. and Method*, **A397**, 354 (1997).
- [6] Y. Abe and N. Morishima: *Nucl. Instr. and Method* **A459**, 256 (2001).
- [7] N. Morishima and M. Sakakibara: *J. of Neutron Res.*, **8**, 233 (2000).
- [8] Y. Abe and N. Morishima: *Nucl. Instr. and Method*, **A481**, 414 (2002).
- [9] N. Morishima and D. Mizobuchi: *Nucl. Instr. and Method*, **A350**, 275 (1994).
- [10] N. Morishima and A. Nishimura: *Nucl. Instr. and Method*, **A426**, 638 (1999).
- [11] N. Morishima and Y. Matsuo: *Nucl. Instr. and Method*, **A490**, 308 (2002).
- [12] N. Morishima: *Ann. Nucl. Energy*, **27**, 505 (2000).
- [13] N. Morishima and Y. Nishikawa: *Ann. Nucl. Energy*, **31**, 737 (2004).
- [14] Y. Matsuo, N. Morishima and Y. Nagaya: *Nucl. Instr. and Method*, **A496**, 446 (2003).
- [15] N. Morishima and Y. Sakurai: *Nucl. Instr. and Method*, **A490**, 527 (2002).
- [16] N. Morishima and T. Mitsuyasu: *Nucl. Instr. and Method*, **A517**, 295 (2004).
- [17] T. Mitsuyasu, N. Morishima and Y. Nagaya: *Nucl. Instr. and Method*, **A537**, 610 (2005).
- [18] Y. Edura and N. Morishima: *Nucl. Instr. and Method*, **A534**, 531 (2004).
- [19] Y. Edura and N. Morishima: *Nucl. Instr. and Method*, **A560**, 485 (2006).
- [20] Y. Edura and N. Morishima: *Nucl. Instr. and Method*, **A545**, 309 (2005).
- [21] H. R. Glyde: *J. Low Temp. Phys.*, **87**, 407 (1992); also *Phys. Rev.*, **B45**, 7321 (1992).
- [22] J. A. Young and J. U. Koppel: *Phys. Rev.*, **135**, A603 (1964).
- [23] M. Nelkin: *Phys. Rev.*, **119**, 741 (1960).
- [24] H. C. Honeck: *Trans. Am. Nucl. Soc.*, **5**, 47 (1962).
- [25] J. R. Beyster: *Nucl. Sci. Eng.*, **31**, 254 (1968).
- [26] N. Morishima: “*ZZ-CLES, Cross section library of moderator materials for low-energy neutron sources*,” NEA Data Bank, NEA-1775 (2006).